

Research Article

Overestimating Impacts of Urbanization on Regional Temperatures in Developing Megacity: Beijing as an Example

Wei Cao ¹, Lin Huang,¹ Lulu Liu,² Jun Zhai,³ and Dan Wu ⁴

¹Key Laboratory of Land Surface Pattern and Simulation, Institute of Geographic Sciences and Natural Resources Research, Chinese Academy of Sciences, Beijing 100101, China

²School of Architecture and Civil Engineering, Chengdu University, Chengdu 610106, China

³Satellite Environment Center, Ministry of Ecology and Environment, Beijing 100094, China

⁴Nanjing Institute of Environmental Sciences, Ministry of Ecology and Environment, Nanjing 210042, China

Correspondence should be addressed to Dan Wu; cumtwudan@163.com

Received 26 September 2018; Revised 14 December 2018; Accepted 13 January 2019; Published 6 February 2019

Academic Editor: Annalisa Cherchi

Copyright © 2019 Wei Cao et al. This is an open access article distributed under the Creative Commons Attribution License, which permits unrestricted use, distribution, and reproduction in any medium, provided the original work is properly cited.

Land-use and land cover changes may have important local, regional, and global climatic impacts by modifying the underlying land surface conditions, which in turn influence the exchange of energy and moisture between the land surface and atmosphere. Many studies have shown that urbanization has contributed to climate warming, and the amount of warming has varied. As the capital of China and one of the world's megacities, Beijing has experienced rapid urbanization over the past 30 years. In this study, we quantitatively investigated the impacts of urbanization on regional temperatures based on observations from meteorological stations and National Centers for Environmental Prediction (NCEP) reanalysis data and overestimating of the impacts were found. Comparing the temperature trends of land-use types, forest showed stronger inhibitory effects on temperature increase ($-0.085^{\circ}\text{C}/10\text{a}$). Cropland also had a negative effect on climate warming yearly and seasonally, especially in winter ($-1.133^{\circ}\text{C}/10\text{a}$) and spring ($-0.299^{\circ}\text{C}/10\text{a}$). Conversely, the urban area showed strong warming effects ($0.438^{\circ}\text{C}/10\text{a}$). The conversion of cropland to urban land appeared to show the highest warming trend ($0.548^{\circ}\text{C}/10\text{a}$). However, the cooling effect of forest and grassland with high vegetation coverage inhibited climatic warming attributed to rapid urbanization. In addition, planting trees or grass along roadsides and increasing green parks and green roofs can also suppress surface warming. Therefore, the actual warming effects of urbanization on temperatures were overestimated in megacities or urban agglomeration regions. The results showed that the green space and landscape configuration should be considered in urban planning to increase green space and reduce the influence of urban heat island effect.

1. Introduction

Increased greenhouse gases represent one of the primary factors underlying global climate change. However, increasing evidence indicates that land-use and land cover (LULC) changes, which fundamentally alter the fluxes of solar and thermal infrared radiation, sensible and latent heat, the movement of water between the subsurface and atmosphere, and the exchange of momentum between the land surface and atmosphere, may also have important local, regional, and global climatic implications [1–3]. In certain cases, the climatic response to LULC changes may exceed the contribution from increasing greenhouse gases [4, 5].

However, fully separating the climatic impacts of LULC changes and global warming is difficult. Climate models such as the community land model (CLM), the community climate system model (CCSM), the dynamic global vegetation model (DGVM), the Lund–Potsdam–Jena model for managed land (LPJmL), the general circulation model (GCM), and the simplified parameterizations primitive equation dynamics model (SPEEDY) were used to simulate, couple, or compare for estimating the effects of LULC on climate change [6–8]. The simulations were based on land cover or vegetation change experiments and comparisons of climatic parameters, such as temperature and precipitation, simulated from actual and potential land-use scenarios.

However, the results varied for the simulation schemes from different models, which may further increase the uncertainties of the study. Many other studies investigated the effects of land-use change on climate primarily via observations from meteorological stations combined with statistical data or remote sensing images [9–12]. However, field data have limited coverage, and there are uncertainties associated with observations from satellites.

Urbanization has increased the surface areas available for absorbing solar energy [13], which may induce a large warming bias in regional or local temperature [14–21]. This can affect the formation of the urban heat island (UHI) [22, 23], which impacts local, regional, and even global climate [24–26]. Gallo et al. evaluated the diurnal temperature range (DTR) at weather observation stations with respect to the predominant LULC and found that stations associated with rural-related LULC typically displayed the greatest observed DTR, whereas stations associated with urban-related LULC displayed the lowest observed DTR. In addition, the warming trend caused by urbanization was 0.06°C per century [9]. Hansen et al. compared surface air temperature changes that occurred in the United States and globally from 1900 to 2000, and they reclassified rural, small town, and urban stations based on satellite measurements of night light intensity instead of population. Their results indicated that the warming trend caused by urbanization was 0.15°C per century [10]. Thus, the results differed significantly depending on whether population data or satellite measurements of night lights were used to classify urban and rural areas. Additionally, the definition of urban and rural stations based on population differed considerably among countries, and light intensity varied significantly among regions in various stages of economic development.

Kalnay et al. proposed the observation minus reanalysis (OMR) method, which used the difference between trends in the observed surface temperatures and the corresponding trends in a reconstruction of the surface temperatures based on a reanalysis of the global weather to estimate the impact of land-use changes on surface warming [24]. The OMR was developed because of the lack of surface observations of temperature, moisture, and wind over land in the National Centers for Environmental Prediction (NCEP)-National Center for Atmospheric Research (NCAR) 50-year reanalysis (NRR) dataset. However, atmospheric vertical soundings of wind and temperature strongly influence the NRR, and surface temperatures were estimated from the atmospheric values. As a result, OMR has the ability to remove the signals of large-scale temperature variations induced by greenhouse gases while retaining the local signals [24]. Based on the OMR method, Kalnay et al., Mario et al., and Nayak et al. investigated the impacts of LULC changes on climate changes in the United States, Argentina, and western India [27–29]. Lim et al. investigated the sensitivity of surface climate change to land types over the Northern Hemisphere and found that surface warming was higher in areas that are barren, anthropogenically developed, or covered with needle-leaf forests, whereas surface warming appeared to be suppressed in highly vegetated areas [30]. These aforementioned studies confirmed the robustness of

the OMR method for detecting nonclimatic changes at the station level and providing a quantitative estimate of additional warming trends associated with LULC changes.

In China, a number of studies related to the warming effects of urbanization have been performed [31–34]. However, most of these studies were on a global, country, or regional scale, and city-scale studies were infrequent. In this study, we apply the OMR method to quantitatively investigate the impacts of urbanization on regional temperatures based on observations from meteorological stations and NCEP reanalysis data, taking Beijing as an example. The study aimed to investigate the overestimation or underestimation of the effects of urbanization on regional temperatures.

2. Materials and Methods

2.1. Study Area. Beijing, both China's capital and one of the world's megacities, has experienced rapid urbanization over the past 30 years. Because of the city's expansion, the land use has changed considerably, with many croplands converted to urban areas. In 2015, Beijing had an area of $16,410\text{ km}^2$ and a population of 21.70 million. Beijing has a dry, monsoon-influenced humid continental climate. The monthly daily average temperature is -3.7°C in January and 26.2°C in July. The precipitation averages approximately 570 mm annually, with approximately three-fourths of the total occurring from June to August. The primary vegetation zone in Beijing is warm temperate deciduous broad-leaved forest.

2.2. Meteorological Observations. The meteorological observation data in China are primarily sourced from the China Meteorological Data Service Center (<http://data.cma.cn/>), where daily data are collected for temperature, precipitation, pressure, evaporation, wind direction, wind speed, and sunshine duration from 756 national basic meteorological stations throughout mainland China. However, the station density is sparse, and only 2 national basic stations are located in Beijing. In addition to the national basic stations, we also collected daily temperature data from 17 other local meteorological stations from rural counties around Beijing provided by the Beijing Meteorological Service. All 19 meteorological stations have formed a relatively dense weather observation network, and periodic continuous observations have been conducted over a long period (Figure 1, Table 1). The daily temperature dataset covered the period from 1979 to 2010. Repeated verifications and quality controls such as data consistency validations, abnormal value elimination, and empty value filling were conducted by the data provider. We aggregated the daily observations into monthly, seasonal, and annual mean values, and the seasonal and annual anomalies were calculated by removing the 32-year (1979–2010) mean annual cycle.

2.3. Reanalysis Data. The monthly reanalysis temperature data were obtained from the National Centers for

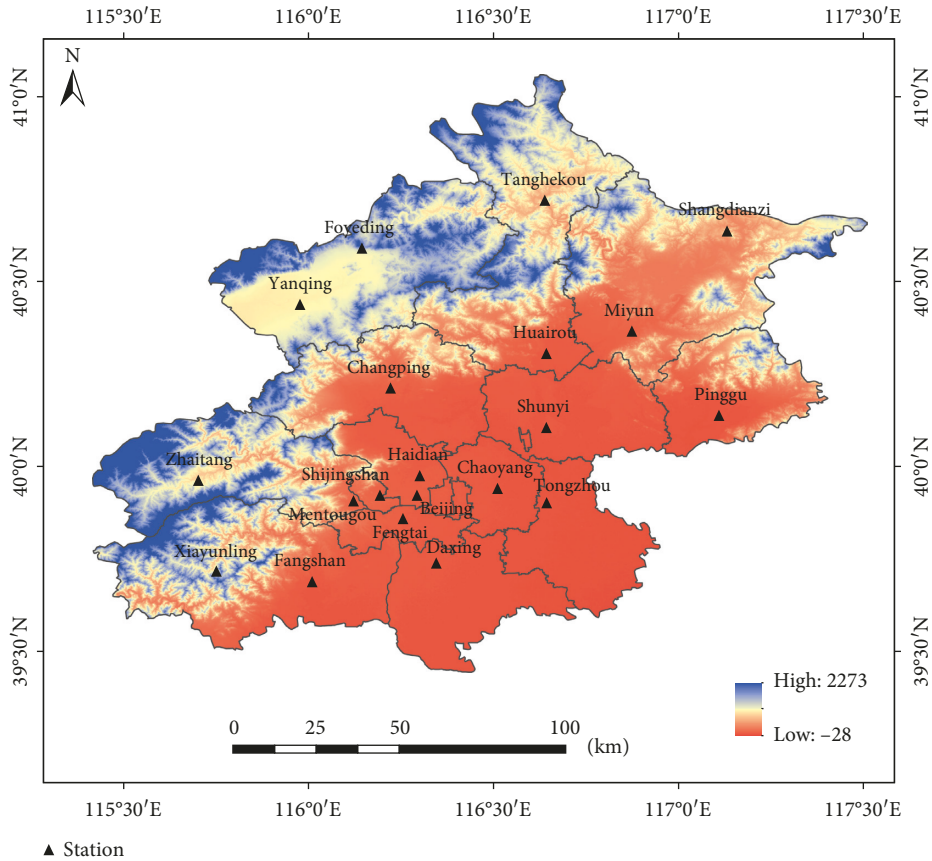


FIGURE 1: Distribution of meteorological stations in Beijing.

TABLE 1: Meteorological stations in Beijing.

Stations	Relocation time
Foyeding	No relocation
Tanghekou	No relocation
Zhaitang	No relocation
Shangdianzi	No relocation
Miyun	No relocation
Mentougou	No relocation
Pinggu	2003
Shunyi	1999
Shijingshan	1997
Huairou	1996
Xiyunling	No relocation
Changping	No relocation
Tongzhou	No relocation
Haidian	No relocation
Fengtai	No relocation
Daxing	2003
Fangshan	2002
Chaoyang	2007
Beijing	1997

Environmental Prediction/Department of Energy (NCEP_DOE) Atmospheric Model Intercomparison Project (AMIP)-II Reanalysis (R-2) ($1.9^\circ \times 1.9^\circ$) covering a period from January 1979 to December 2010, which represented an updated and human error-corrected version of the NCEP-NCAR reanalysis (R-1) dataset [35, 36]. For each

meteorological station, the monthly mean R-2 temperatures were interpolated to their location (longitude and latitude) using a bilinear interpolation method. Then, the seasonal and annual mean values were aggregated from the monthly value. Similar to the observational data, seasonal and annual anomalies were calculated by removing the 32-year (1979–2010) mean annual cycle. To ensure the reliability of the R-2 data, we assessed the performance of the R-2 temperatures relative to the observational data. The annual anomalies for the observations and R-2 data were compared, and a good correlation was observed for the interannual variability (Figure 2). The maximum correlation coefficient was 0.86 at the Foyeding station, and the minimum correlation coefficient was 0.52 at the Tongzhou station (Table 2).

2.4. LULC Data in 1990, 2000, and 2010. Quantitative analysis of the effects of LULC change on temperature at a city scale has rarely been performed, and raster data with $1\text{ km} \times 1\text{ km}$ or coarser spatial resolution were typically used. Thus, capturing LULC changes at the city scale is difficult, and additional detailed vector data are required to support the research. In this study, LULC data at a 1 : 100,000 scale in 1990, 2000, and 2010 were collected from China’s Land-Use/Cover Datasets (CLUDs), which were provided by the National Resources and Environmental Scientific Data Center (RESDC) of the Chinese Academy of Sciences (CAS).

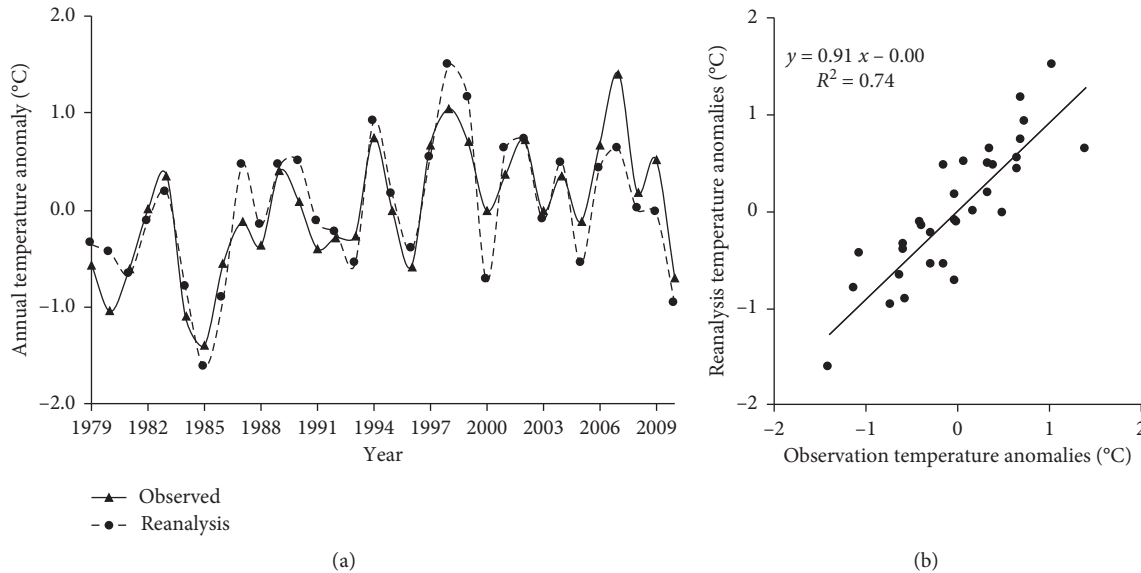


FIGURE 2: Correlation between the observed temperature anomalies and the reanalysis temperature anomalies at the Foyeding station.

TABLE 2: Correlation coefficients of the observed temperature anomalies and the reanalysis temperature anomalies at the meteorological stations in Beijing.

Stations	Correlation coefficient
Foyeding	0.86
Tanghekou	0.81
Zhaitang	0.80
Shangdianzi	0.83
Miyun	0.77
Mentougou	0.75
Pinggu	0.77
Shunyi	0.79
Shijingshan	0.75
Huairou	0.74
Xiayunling	0.77
Changping	0.68
Tongzhou	0.52
Haidian	0.67
Fengtai	0.64
Daxing	0.73
Fangshan	0.77
Chaoyang	0.71
Beijing	0.74

These data were classified as farmland, forestland, grassland, built-up land, water body, and unutilized land according to the resources and utilization property. These data were produced by human-computer interactive interpretations of Landsat Thematic Mapper (TM) digital images. For areas not covered by Landsat TM data or covered by poor quality data, supplemental data were used from the CCD multi-spectral data from the Huanjing-1 satellite (HJ-1). After interpretations were performed, nationwide field surveys were conducted predominantly in fall for northern China and spring for southern China. The accuracy of the 6 land-use classes was above 94.3%, which met the required user mapping accuracy at the 1:100,000 scale [37–39]. In this study, the LULC dataset in Beijing was extracted from

CLUDs using ArcMap 10.3, and the first four land-use types (farmland, forestland, grassland, and urban land) would be discussed.

2.5. Station Classification Scheme. To quantify the effects of LULC change on climate, we classified the stations associated with different LULCs according to the workflow shown in Figure 3. First, we extracted LULC data in 1990, 2000, and 2010 for buffer zones with a radius of 3 km [32] centered at each meteorological station (Figure 4). Second, we calculated the areal ratios of LULC to the buffer zone of each station. Finally, we calculated the LULC ratio changes for 1990–2000 and 2000–2010 (Figure 5). When the areal fraction change of any land cover for a given station was greater than 20%, it was defined as a station with dramatic LULC changes; otherwise, it was designated as a station with stable LULC types. For the stable stations, if the areal fraction of any land cover in the 3 km buffer zone exceeded 70%, that land cover type was considered to be the dominant land cover type with the greatest influence on temperature changes adjacent to the station.

The positions of eight stations (Table 1) were changed, which would change the underlying surface of the meteorological stations and affect observation records. Therefore, only stable stations without relocation were applied for station classification.

According to the classification scheme, six stable stations (SS) and five changed stations (CS) were selected from all the stations (Tables 3 and 4). The SS included forestland, urban land, and mixed type stations, and the LULC changes of CS were primarily converted from farmland to urban land. However, there were no stations that could represent cropland stations according to the criterion. Cropland was the second largest land-use type in Beijing; therefore, it was important to investigate its impact on regional climate change. In 1990, the dominant land-use type surrounding

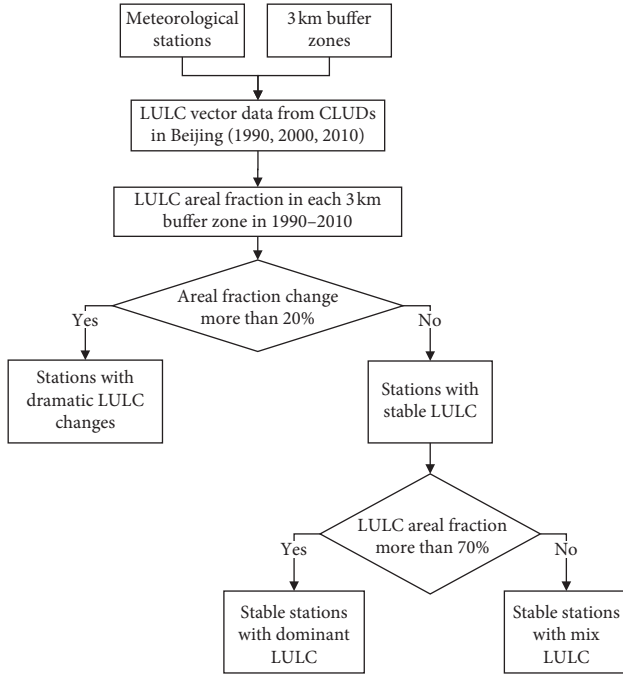


FIGURE 3: Station classification workflow.

the stations of Daxing and Pinggu was cropland, and the areal proportion of cropland in the 3 km buffer zones was 73% and 77%, respectively. Although much of the cropland around the two stations was changed to urban land after 1990, in order to make the best use of the available information, we selected Daxing and Pinggu as the representative stations for cropland during 1979–1990 (Table 3).

2.6. Observation Minus Reanalysis Method. Many studies have shown that the OMR analysis method proposed by Kalnay and Cai can better reflect the impact of LULC change on climate; thus, this method was used for our study. Based on temperature data from 1979 to 2010, firstly, we calculated the annual and seasonal average temperature anomalies for the observed and reanalyzed temperature. Then, we calculated the trend of the temperature anomalies for the observed and reanalyzed temperature, respectively, using the linear trend analysis method, which was written as follows:

$$t_{\text{slope}} = \frac{n \times \sum_{j=1}^n j \times t_j - \sum_{j=1}^n j \times \sum_{j=1}^n t_j}{n \times \sum_{j=1}^n j^2 - \left(\sum_{j=1}^n j\right)^2}, \quad (1)$$

where t_{slope} represents the temperature anomaly trends of reanalysis (t_{rea}) and observation (t_{obs}), n is the number of years, and t_j is each reanalysis or observed year temperature anomaly.

Finally, we calculated the OMR temperature trends as follows:

$$T_{\text{OMR}} = T_{\text{rea}} - T_{\text{obs}}, \quad (2)$$

where T_{OMR} is the temperature trends of OMR temperature; T_{rea} is the temperature trends of reanalyzed temperature; and T_{obs} is the temperature trends of observed temperature.

The temperature trend is not only related to the type but also the area of the land cover types or changes. In this study, we did not use the traditional averaged temperature trend from all meteorological stations applied in previous studies; instead, we used the area-weighted temperature trend of the entire study area because it could better reflect regional climate changes. Formula is calculated as

$$T = \frac{\sum_{i=1}^j (T_i \times A_i)}{A}, \quad (3)$$

where T is the area-weighted temperature trend; T_i is the temperature trend of a typical LULC or LULC change, such as the forest temperature trend or the temperature trend of the LULC change from cropland to urban land; A_i is the area of the typical LULC or LULC change; and A is the total area of the entire region.

3. Results

3.1. Temperature Changes over the Last 30 Years. From 1979 to 2010, the observed annual mean temperature fluctuated with an upward trend. From the 1980s to 1990s, the observed temperature had a larger increase of 0.69°C, whereas from the 1990s to 2000s, the observed temperature had a smaller increase of 0.12°C (Figure 6(a)). Conversely, the reanalyzed annual mean temperature had a different fluctuation compared with the observed temperature (Figure 6(b)). The reanalyzed temperature change fluctuated upwards, with an increase of 0.62°C from the 1980s to 1990s but declined by 0.38°C from the 1990s to 2000s.

Figure 7 showed the observed, reanalyzed, and OMR temperature anomaly trends for each station. For the observed temperature (Figure 7(a)), all stations presented remarkable warming trends with an average of 0.463°C/10a. Spatially, stations in the suburban area showed a larger increase in temperature, and the nearest suburban stations to the city center, such as Daxing, Tongzhou, and Shunyi exhibited the most significant warming trends, with values of 0.95°C/10a, 0.93°C/10a, and 0.85°C/10a, respectively. These trends were higher than those of stations in the urban area, such as Shijingshan, Haidian, and Beijing. The warming trends for the Shangdianzi, Zhaitang, Xiayunling, and Tanghekou stations, which were located in rural areas, were not remarkable; Tanghekou station showed the lowest trend of 0.004°C/10a.

For the reanalyzed temperature (Figure 7(b)), all stations showed warming trends, with an average of 0.249°C/10a. Thirteen stations had less remarkable warming trends, with values between 0.14°C and 0.20°C/10a. The higher trends occurred at the Shunyi, Daxing, and Huairou stations, and the Shunyi station trend reached 0.59°C/10a.

For the OMR temperature (Figure 7(c)), the trends were determined by subtracting the data from Figure 7(a) and Figure 7(b). Most stations had higher observed temperature values than the reanalyzed temperatures; thus, the corresponding OMR temperatures primarily exhibited positive values. Only the observed temperature trends in the Xiayunling, Zhaitang, and Tanghekou stations were lower than the reanalyzed temperatures. Therefore, the OMR temperature trends were negative, which indicated a decreasing trend.

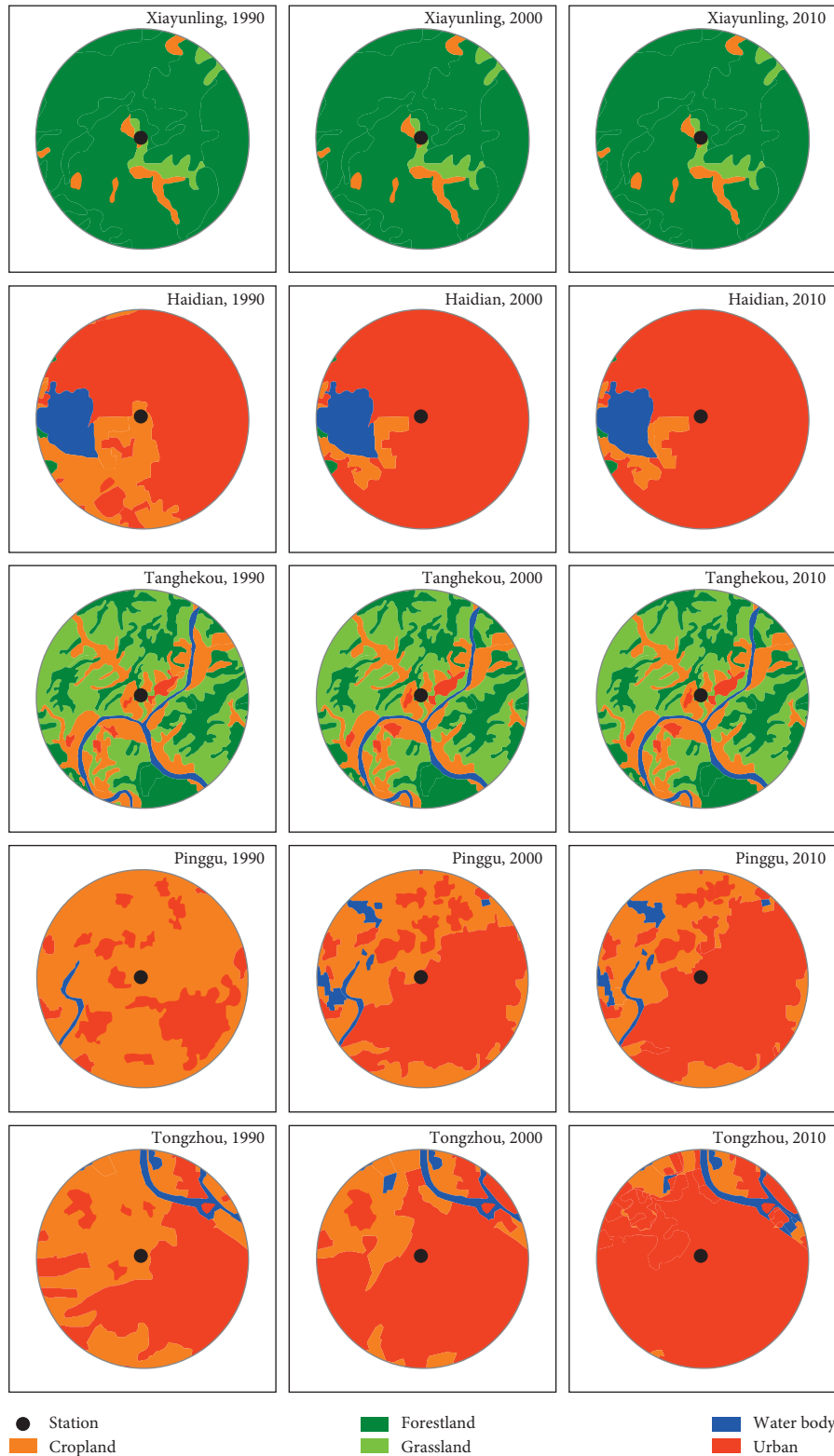


FIGURE 4: LULC in the 3 km buffer zones at the Xiayunling, Haidian, Tanghekou, Pinggu, and Tongzhou stations in 1990, 2000, and 2010.

3.2. Effects of Urbanization and Nonurbanization on Local Temperatures. To investigate how different land cover types influenced local temperatures, we averaged the annual and seasonal OMR trend groups by the dominant land cover of SS. Additionally, to reflect the average temperature trend, we

calculated the average trend of all 19 stations to obtain a background value (BV) for the temperature change. Forestland, urban area, mixed type, and BV were computed in the period of 1979–2010. And cropland was computed in the period of 1979–1990. The results are shown in Table 5.

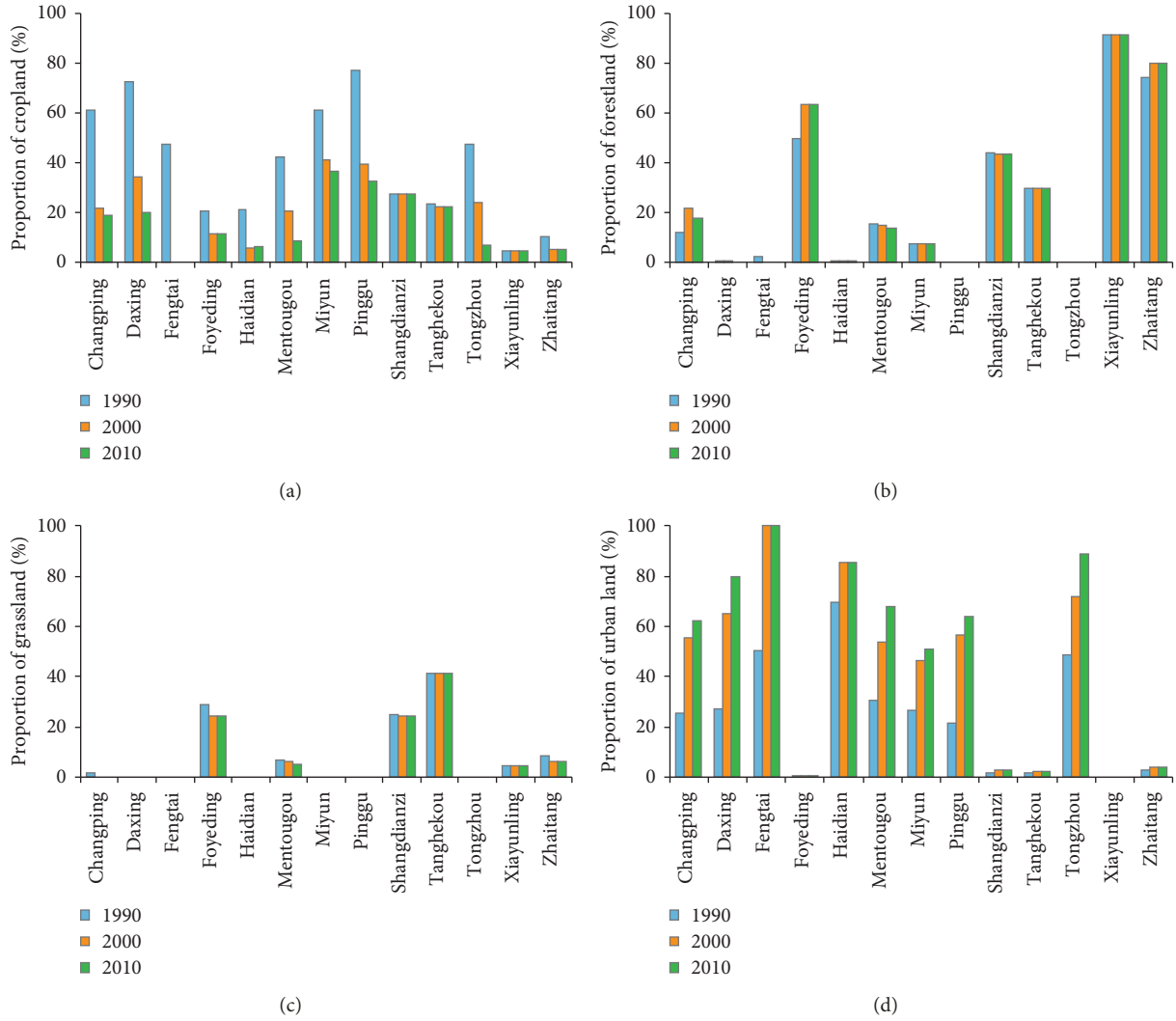


FIGURE 5: Area proportion of LULC in the 3 km buffer zones around each meteorological station from 1990 to 2010. (a) Cropland proportion. (b) Forestland proportion. (c) Grassland proportion. (d) Urban land proportion.

TABLE 3: Stable stations and dominant LULC in Beijing.

Dominant LULC types	Representative stations	Areal fractions of dominant LULC types
Forestland	Zhaitang	80%
	Xiayunling	91%
Urban land	Haidian	80%
	Foyeding	99% (forestland 63%, grassland 24%, and cropland 12%)
	Shangdianzi	95% (forestland 44%, grassland 24%, and cropland 27%)
Mixed forestland, grassland, and cropland	Tanghekou	93% (forestland 30%, grassland 41%, and cropland 22%)
Cropland	Daxing	73%
	Pinggu	77%

The seasonal OMR temperature trends of forestland varied considerably. In summer and autumn, the OMR temperatures showed decreasing trends. However, in spring

TABLE 4: Stations with dramatic LULC changes in Beijing.

Primary LULC change	Representative stations	Areal fractions of primary LULC change from 1990 to 2000	Areal fractions of primary LULC change from 2000 to 2010
Cropland to urban	Miyun	20.2%	4.5%
	Tongzhou	22.9%	17.0%
	Changping	30.1%	6.9%
	Mentougou	23.0%	14.4%
	Fengtai	49.5%	0

and winter, the OMR temperatures showed increasing trends. The decreasing trends were higher than the increasing trends; thus, the annual OMR trends of the forestland also showed decreasing trends, with a value of $-0.085^{\circ}\text{C}/10\text{a}$. Additionally, compared with the BVs, both the seasonal and annual forestland trends were lower, which indicated that forestland inhibited a temperature increase.

For the cropland, the annual and seasonal OMR trend values were negative, which indicated that cropland had a

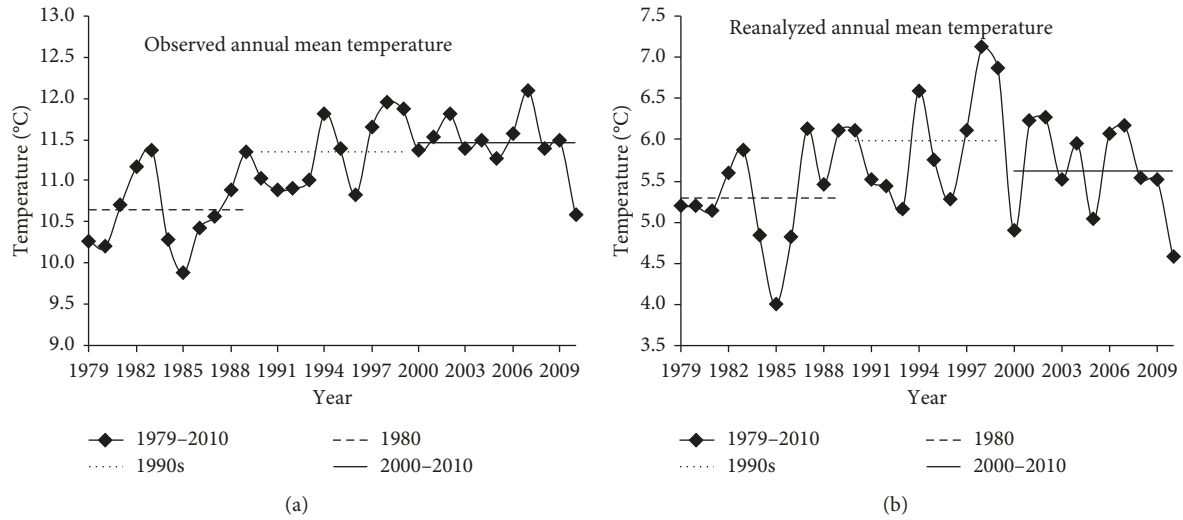


FIGURE 6: Time series of the observed (a) and reanalyzed (b) annual mean temperatures from 1979 to 2010.

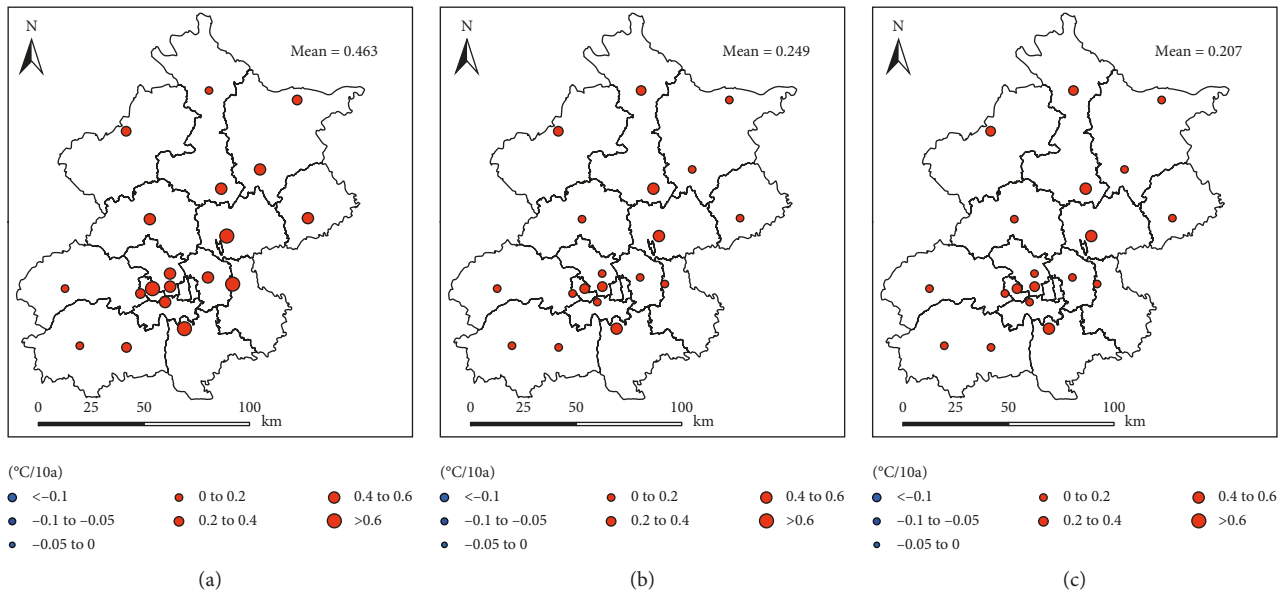


FIGURE 7: Observed (a), reanalyzed (b), and OMR (c) annual mean temperature trends in Beijing from 1979 to 2010.

TABLE 5: Linear trend of the OMR annual and seasonal mean temperatures for the primary LULC in Beijing ($^{\circ}\text{C}/10\text{a}$).

LULC	Annual	Spring	Summer	Autumn	Winter
Forestland	-0.085	0.055	-0.294	-0.226	0.118
Cropland	-0.114	-0.299	-0.038	-0.224	-1.133
Urban area	0.438	0.592	0.212	0.231	0.626
Mixed types (forestland, grassland, and cropland)	0.025	0.078	-0.176	-0.063	0.205
BV	0.207	0.351	0.041	0.081	0.243

strong inhibiting effect on climate warming. The annual OMR trend was $-0.114^{\circ}\text{C}/10\text{a}$, which was the lowest among the 4 dominant land-use types shown in Table 5. In winter and spring, the inhibiting impacts on climate warming

were the most remarkable, and the OMR trend values were $-1.133^{\circ}\text{C}/10\text{a}$ and $-0.299^{\circ}\text{C}/10\text{a}$, respectively.

For the urban area, the annual OMR temperature trend was $0.438^{\circ}\text{C}/10\text{a}$, which was the highest among the 4 types. All OMR temperatures in the four seasons showed increasing trends, and the trend values in summer and autumn were lower than those in spring and winter. In addition, all the trend values were much higher than the BVs. As a result, the urban area showed strong warming effects on temperature changes.

For the mixed land cover combining forestland, grassland, and cropland, the annual OMR temperature showed an increasing trend; however, the trend was low ($0.025^{\circ}\text{C}/10\text{a}$). The seasonal OMR temperature changes were similar to that of forestland in summer and autumn, which showed decreasing OMR temperatures trends. In spring and winter,

increasing OMR temperatures trends were observed. The annual and seasonal trend values were much lower than the BVs. Hence, the mixed land cover also inhibited temperature increases.

The dominant LULC change in Beijing from 1990 to 2010 was from farmland to urban land, with 742.3 km² converted from 1990 to 2000, which accounted for 65.5% of the total conversion area, and 489.4 km² converted from 2000 to 2010, which accounted for 80.6% of the total conversion area for this period (Figure 8). Therefore, five changed stations (CSs) were selected to analyze the effects of urbanization on local temperatures. Table 6 shows the OMR temperature change trends of the five CSs. The results showed that as urbanization dramatically increased over the past 20 years (1990–2010), the OMR annual temperatures for all stations showed increasing trends, and the trend values were much higher than the entire study period (1979–2010). These findings indicated that the warming effect was enhanced as the farmland was converted to urban land. From 1990 to 2010 when intense LULC changes occurred, the temperature trend during the first decade (1990–2000) was much higher than that during the second decade (2000–2010), which indicated that the warming trend was slowing down. This decrease may have been due to decreases in the conversion area from cropland to urban area. We analyzed the relationship between the proportion of changed area and the annual OMR temperature trends from 1990 to 2000 and 2000 to 2010 (Figure 9). The results showed a positive correlation, with a higher conversion rate from farmland to urban area corresponding to a higher temperature trend.

3.3. Combined Effects of Land Cover Types and Urbanization on Regional Temperature Change. The unchanged (Figure 10(a)) and changed (Figure 10(b)) land cover areas for 1990–2010 were integrated into one map (Figure 10(c)) based on the following 6 categories: unchanged forest (UF), unchanged cropland (UC), unchanged urban area (UU), unchanged water area (UW), unchanged mixed type (UM) (combination of forestland, grassland, and cropland), and urbanization from cropland (CCU). The area of UW was small and was not been considered.

The Fishnet tool in ArcMap 10.3 was used to create a net of rectangular cells with predefined size. In this study, the cell size was 6 km, and the area of each fishnet cell was close to the aforementioned buffer zone (centered at the station location with a 3 km radius) in Section 2.5. An intersecting analysis was performed between the integrated map and the fishnet, and the area percentage of UF, UC, UU, UM, and CCU in each cell was calculated to identify the predominant type for each cell for the classification.

Based on the results in Tables 5 and 6, the temperature changing trend was set for each cell in Figure 10(c), and the area-weighted OMR trend (AW-OMR) (Table 7) of the entire Beijing area was calculated using the area-weighted method presented in equation (3).

The UF covered the largest area in Beijing, but its AW-OMR was only $-0.034^{\circ}\text{C}/10\text{a}$, which was the lowest among

the 5 categories in Table 7. The UC covered 22.3% of the area in Beijing, and its AW-OMR was also negative ($-0.025^{\circ}\text{C}/10\text{a}$). The AW-OMRs of UU, UM, and CCU were all positive, but the AW-OMRs of UU and UM were only $0.007^{\circ}\text{C}/10\text{a}$ and $0.006^{\circ}\text{C}/10\text{a}$, respectively, which seemed to have a considerably lower impact on climate warming in Beijing. For UU, the areal ratio was the lowest; thus, the warming impact of UU was also very low, although the OMR trend of UU was the second largest. For UM, the areal ratio was the second largest, but the temperature increase was the lowest, so the UM also had little impact on regional climate warming in Beijing. The AW-OMR of CCU was the largest, nearly twice that of the UF. However, the areal ratio of CCU was only 12.2%, which was nearly one-third that of the UF and one-half that of the UC. These results indicated that UF and UC had considerable inhibiting effects on temperature increase in Beijing, and the CCU contributed greatly to climate warming. In contrast, the warming impact of UU and UM can be ignored.

4. Discussion

4.1. Climate Effects of Land Cover and Vegetation Coverage. Different land cover types showed varying trends of temperature change in Beijing, which were consistent with the results of Fall et al. and Lim et al., who found that surface warming was greater for areas that are barren or anthropogenically developed, whereas surface warming appeared to be suppressed by highly vegetated areas [3, 30]. Satellite observations of the GIMMS NDVI dataset at 16-day intervals from 1982 to 2006 showed that the annual and summer mean NDVI of all stations, which were extracted using the bilinear sampling method at each station, were in the following sequence: forest > mixed land cover > farmland > urban land (Figure 11). The annual mean NDVI and NDVI trend were negatively correlated with the OMR temperature trend, and the correlation ratio was -0.42 and -0.78 , respectively (Figure 12). Higher levels of vegetation coverage correspond to stronger transpiration, and the additional radiation energy would be partitioned into latent heat, and the sensible heat would be low. Therefore, as the NDVI increased, the OMR temperature showed a decreasing trend.

Based on the above findings, we further revealed that the declining trend of the average annual temperature of broad-leaved deciduous forest was primarily due to the strong cooling trend in summer and autumn. The differences in the temperature trends among the four seasons were also partially related to the variations in vegetation coverage and precipitation. In summer, precipitation was higher than that in other seasons, and soil moisture would also be higher; therefore, most of the radiative energy would be absorbed at the ground surface and used for physical evaporation and transpiration of water. Thus, the partitioned latent heat would be higher while the sensible heat would be lower, which could explain why the temperature trend was lower in the wet season.

Forestland and grassland showed stronger inhibitory effects on temperature increases relative to other land cover types, and the continuous implementation of ecological

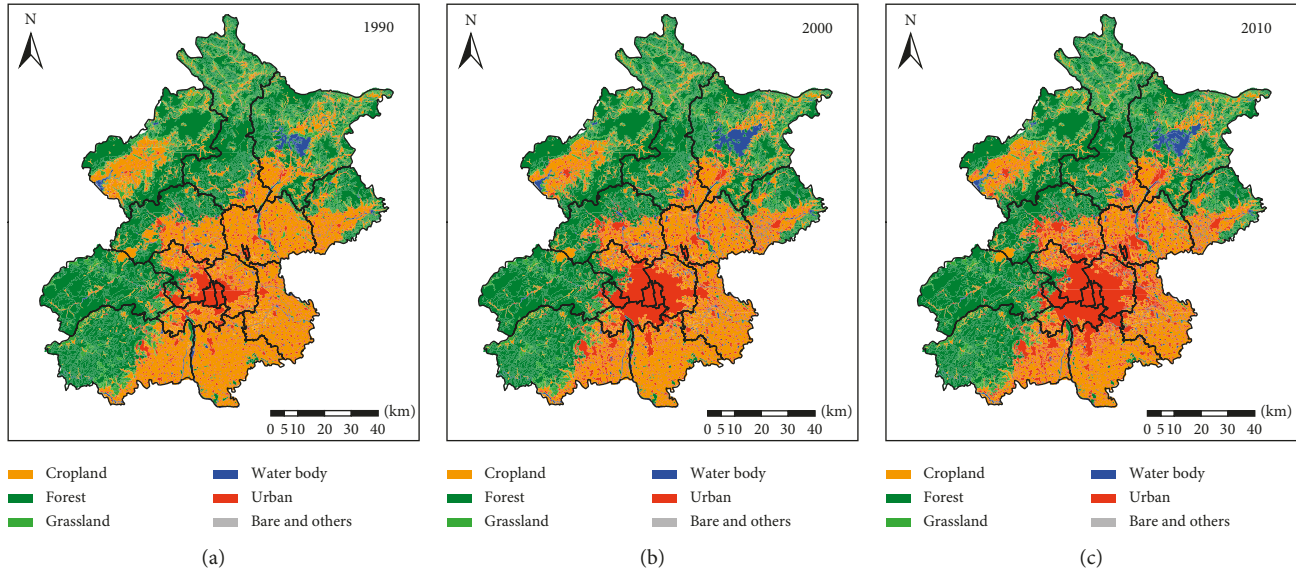


FIGURE 8: Land-use and land cover distribution in Beijing from 1990 to 2010.

TABLE 6: Trends of OMR annual mean temperature of the urbanization stations ($^{\circ}\text{C}/10\text{a}$).

Stations	1979–2010	1990–2010	1990–2000	2000–2010
Miyun	0.246	0.421	0.441	0.048
Tongzhou	0.786	0.882	1.139	0.485
Changping	0.310	0.630	0.852	0.309
Mentougou	0.174	0.379	0.299	0.136
Fengtai	0.350	0.426	0.634	0.152
Average	0.373	0.548	0.673	0.226

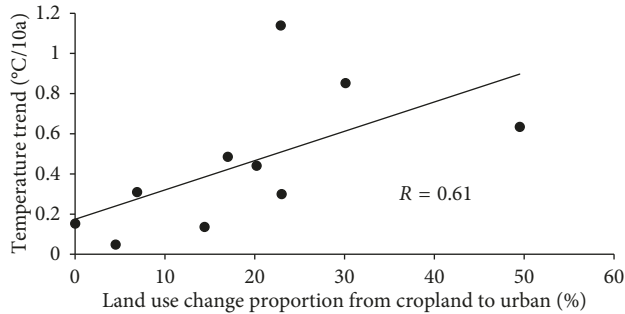


FIGURE 9: Correlation between urbanization proportions and OMR temperature trends.

restorations in Beijing may play an important role in their effects. To improve and optimize the ecological and environmental conditions of Beijing, Tianjin, and surrounding areas; protect forest and grass vegetation; and restrain desertification expansion, the Chinese government launched the Beijing-Tianjin sandstorm source control project in 2001. In Beijing, 6 rural counties, including Mentougou, Huairou, Miyun, Yanqing, Pinggu, and Changping, were involved in this project. From 2001 to 2010, reforestation by planting and aerial seeding covered $1.24 \times 10^5 \text{ hm}^2$ of mountainous area, and the sparsely forested land closed for natural regeneration totaled $1.12 \times 10^5 \text{ hm}^2$. Nearly 7900 people had emigrated from the mountainous region to

suburban areas, thereby reducing anthropogenic activities and disturbances on these fragile ecosystems [40]. For forest and grassland, although the land cover was not changed, the vegetation coverage of these areas had been greatly increased because of ecological restoration programs. Such changes in vegetation likely led to the inhibiting effects on increase in temperature for these areas.

Cropland had a strong inhibiting effect on temperature increase, especially in spring and winter. In spring, precipitation was less abundant and was insufficient for crop growth, so most of the crops required irrigation, especially for winter wheat. Irrigation allowed more energy to be partitioned into latent heat than into sensible heat, which caused the cooling effect. In winter, from the observations of the two representative stations (Pinggu and Daxing), the maximum snow depth increased during 1979–1990, which would cause an increase in surface albedo and lead to decreased net radiation and temperature.

To inhibit the warming rate, continuous implementation of ecological restoration projects had been shown to be effective by increasing the regional vegetation coverage and forest canopy density (Figures 11 and 12). Higher vegetation coverage corresponds to greater transpiration, and more radiation energy will be partitioned into latent heat, which will suppress the surface warming [3, 6, 30, 41, 42]. Additionally, greening projects in urban areas, such as planting vegetation along roadsides, increasing green spaces, can also limit surface warming. Meanwhile, the coverage of green vegetation can protect impervious surface from solar radiation, thereby reducing the net solar radiation absorbed by the surface, and less surface heat will be transported to the atmosphere [43–45].

4.2. *Overestimating Impacts of Urbanization on Regional Temperatures.* Land cover that changed from cropland to urban area showed the highest warming trend, which may be

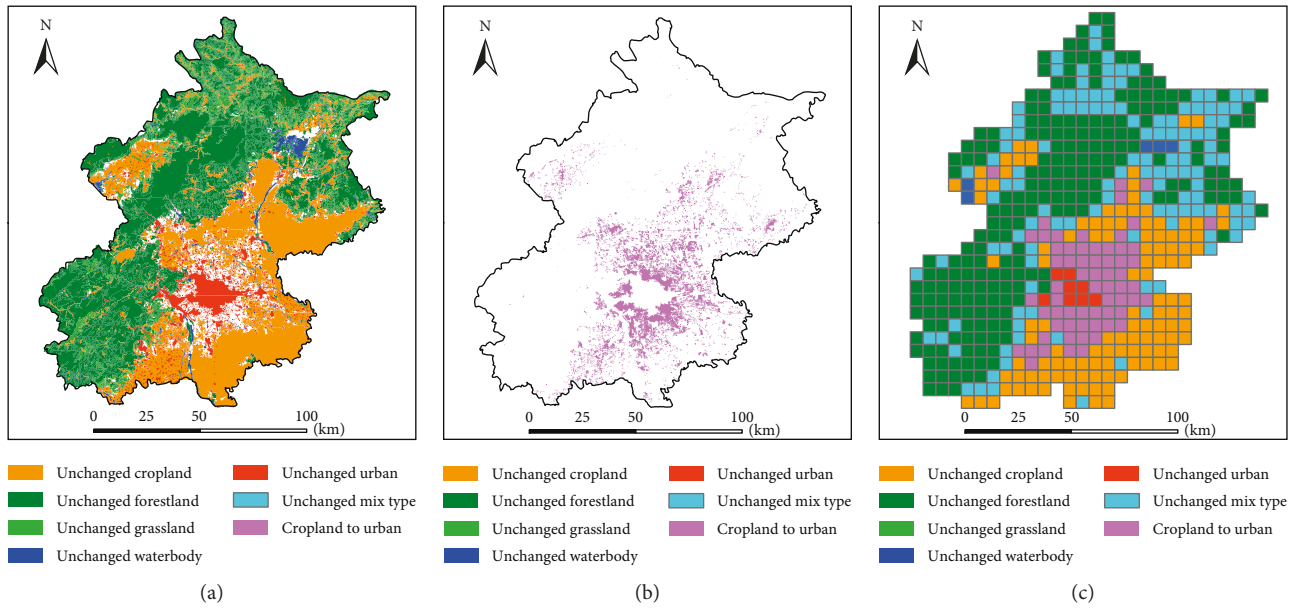


FIGURE 10: Unchanged land cover types, urbanization, and integrated map from 1990 to 2010.

TABLE 7: Area-weighted OMR temperature trend in Beijing from 1990 to 2010.

Type	OMR trend	Pixel amount of each type (ratio)	Area-weighted OMR trend of each type (AW-OMR)	Area-weighted OMR trend in Beijing
Unchanged forest (UF)	-0.085	211 (40.3%)	-0.034	0.020
Unchanged cropland (UC)	-0.114	117 (22.3%)	-0.025	
Unchanged urban area (UU)	0.438	8 (1.5%)	0.007	
Unchanged mix type (UM)	0.025	124 (23.7%)	0.006	
Urbanization from cropland (CCU)	0.548	64 (12.2%)	0.067	

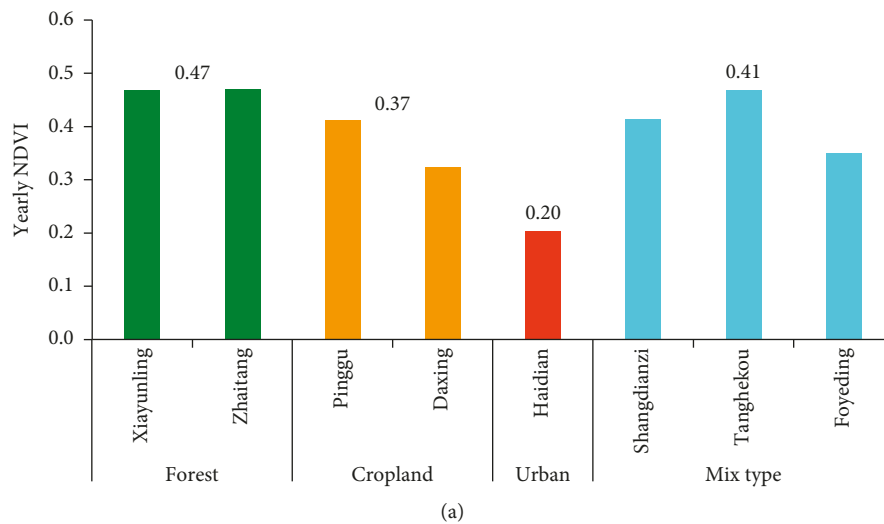


FIGURE 11: Continued.

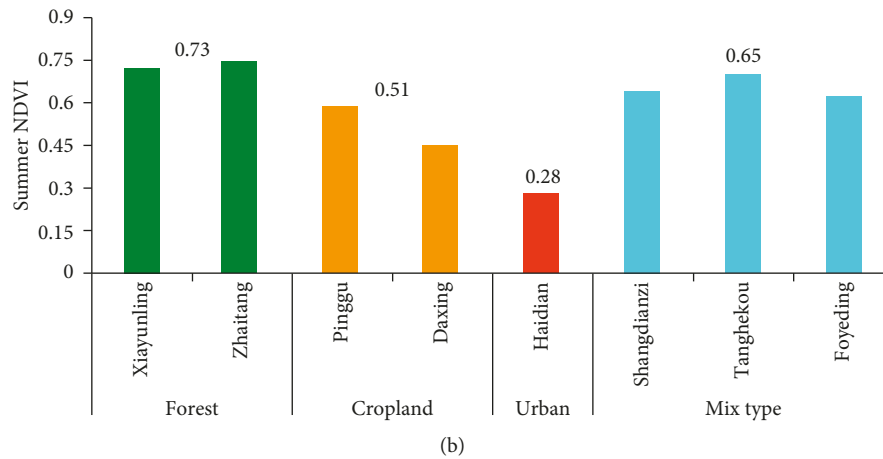


FIGURE 11: Annual and summer mean NDVI of typical stations from 1982 to 2006.

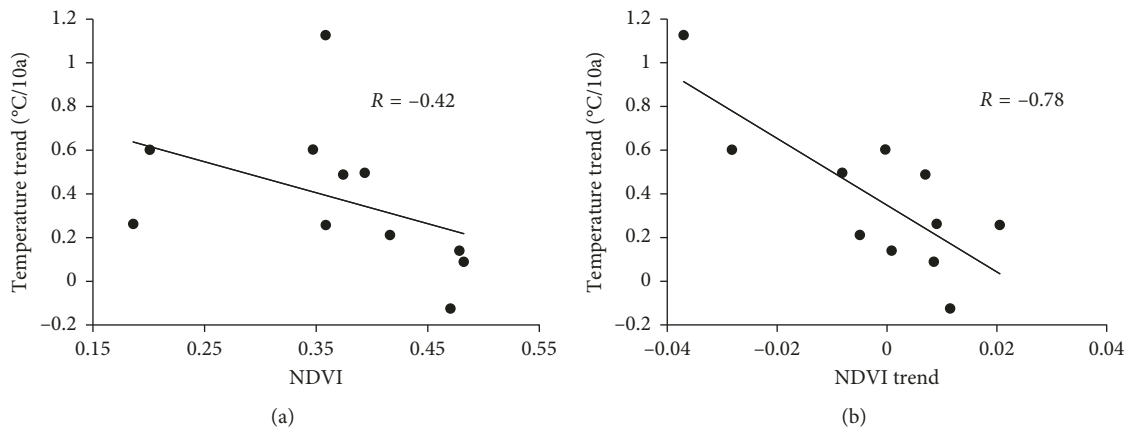


FIGURE 12: Correlation between the temperature trend and the NDVI and NDVI trend.

the result of a decline in vegetation coverage, with the conversion of cropland to urban area and a change in the underlying surface from soil and vegetation to an impervious surface. Impervious surfaces are generally composed of bricks, tiles, concrete, and asphalt. Although these materials have high solar radiation reflectance, they also have more rapid heat transfer and a higher heat-trapping capacity relative to soil [43, 44]. Solar radiation is directly absorbed by the surface, and much of the surface heat is transported to the atmosphere in the form of sensible heat, which leads to a high rate of increasing temperature.

The combined climate effects of land cover and changes measured $0.02^{\circ}\text{C}/10\text{a}$ in Beijing, which indicated that the temperature showed increase trend under rapid urbanization but was far less than that estimated in previous studies [15–17, 31, 32, 45, 46]. Yang et al. found that the mean OMR trend in metropolises and large cities in eastern China was $0.398^{\circ}\text{C}/10\text{a}$ and $0.26^{\circ}\text{C}/10\text{a}$, respectively, from 1981 to 2007 [17]. Zhou et al. found that the OMR maximum and minimum temperature in winter from 1979 to 1998 was $-0.016^{\circ}\text{C}/10\text{a}$ and $0.116^{\circ}\text{C}/10\text{a}$, respectively [31]. Li et al. found an overall warming of $0.142^{\circ}\text{C}/10\text{a}$ in China from 1979 to 2010 [32]. There may be two reasons for the differences between our results and those of the previous

studies. China has experienced rapid urbanization and economic growth since the Chinese economic reform. From 1978 to 2000, the number of small towns soared from 2,176 to 20,312, nearly double that of the world average during this period. The number of cities increased from 190 to 663. The environment surrounding the meteorological stations in China had changed greatly due to urban expansions. Sun et al. found that after the 1980s, 109 national meteorological stations formerly located in rural areas were encroached upon by cities, and an additional 61 stations were near the cities [47]. Most previous studies [17, 31, 32, 47–49] only selected the national meteorological stations for analysis, so the results were greatly influenced by urbanization, and the effects on increased temperature may had been overestimated. In this study, more nonurban stations such as Zhaitang, Foyeding, Xiayunling, Tanghekou, and Shangdianzi were included in this analysis, which can more objectively explain the regional impacts of different LULC types on temperature change. Additionally, previous studies [17, 31, 32, 50, 51] used the arithmetic mean trend of all stations to represent the regional impacts of LULC. In this study, the combined climate effects were estimated with an area-weighted method based on the OMR trend and area proportion of individual LULC and LULC change,

which more accurately reflects the regional climate change. Through the method, the cooling effects of large areas of forestland with high vegetation cover were highlighted. The area-weighted OMR trend was only $0.02^{\circ}\text{C}/10\text{a}$, which indicated that the climate warming trend attributed to rapid urbanization was greatly inhibited.

5. Conclusion

We investigated the combined effects of land cover and urbanization on climate warming using the OMR method in Beijing. Our calculations were based on the meteorological observations, NCEP reanalysis data, and high spatial resolution LULC data. The OMR temperature trend demonstrated that forest and cropland can both inhibit temperature increases. The cooling effect of forest was more remarkable in summer, whereas the cooling effect of cropland was more remarkable in winter. Urban areas showed increasing trends in temperature change. The conversion of cropland to urban areas resulted in the highest warming trend, and higher conversion ratios correspond to more remarkable warming. The combined regional impacts of land cover and urbanization characterized by the AW-OMR trend was only $0.020^{\circ}\text{C}/10\text{a}$. Our results indicate that urbanization was still the main reason for temperature increase, whereas the forest, grassland, and cropland had a remarkable cooling effect in Beijing. Planting vegetation along roadsides and increasing green parks and green roofs can also suppress surface warming. Therefore, in megacities or urban agglomeration regions, the actual warming effects of urbanization on temperatures appeared to be overestimated. Our study showed that green space and landscape configuration should be incorporated into urban planning to increase green space and reduce the influence of urban heat island.

Data Availability

In this paper, we mainly used the meteorological observation data, reanalysis data, and land-use/cover datasets. The meteorological observation data used to support the findings of this study were supplied by the National Meteorological Information Center (<http://data.cma.cn/>) under license and so cannot be made freely available. Requests for access to these data should be made to data@cma.gov.cn. The reanalysis data used to support the findings of this study were supplied by the National Centers for Environmental Prediction/Department of Energy (NCEP_DOE) Atmospheric Model Intercomparison Project (AMIP)-II Reanalysis (R-2) (<http://www.emc.ncep.noaa.gov/>) under license and so cannot be made freely available. Requests for access to these data should be made to cfs@noaa.gov. The land-use/cover datasets used to support the findings of this study were supplied by the National Resources and Environmental Scientific Data Center of the Chinese Academy of Sciences (<http://resdc.cn/>) under license and so cannot be made freely available. Requests for access to these data should be made to xuxl@reis.ac.cn.

Conflicts of Interest

The authors declare that there are no conflicts of interest.

Acknowledgments

This research was funded by the National Key R&D Program of China (nos. 2017YFC0506404 and 2017YFC0506606), National Natural Science Foundation of China (no. 41501484), and Service Project on the Cultivation and Construction for the Characteristic Research Institute, Chinese Academy of Sciences (no. TSYJS05).

References

- [1] N. S. Diffenbaugh, "Influence of modern land cover on the climate of the United States," *Climate Dynamics*, vol. 33, no. 7–8, pp. 945–958, 2009.
- [2] R. Mahmood, R. A. Pielke, K. G. Hubbard et al., "Impacts of land use/land cover change on climate and future research priorities," *Bulletin of the American Meteorological Society*, vol. 91, no. 1, pp. 37–46, 2010.
- [3] S. Fall, D. Niyogi, A. Gluhovsky, R. A. Pielke, E. Kalnay, and G. Rochon, "Impacts of land use land cover on temperature trends over the continental United States: assessment using the North American Regional Reanalysis," *International Journal of Climatology*, vol. 30, no. 13, pp. 1980–1993, 2009.
- [4] National Research Council, *Radiative Forcing of Climate Change: Expanding the Concept and Addressing Uncertainties*, The National Academies Press, Washington, DC, USA, 2005.
- [5] R. Mahmood, R. A. Pielke, K. G. Hubbard et al., "Land cover changes and their biogeophysical effects on climate," *International Journal of Climatology*, vol. 34, no. 4, pp. 929–953, 2013.
- [6] R. Betts, "Biogeophysical impacts of land use on present-day climate: near-surface temperature change and radiative forcing," *Atmospheric Science Letters*, vol. 2, no. 1–4, pp. 39–51, 2001.
- [7] P. J. Lawrence and T. N. Chase, "Investigating the climate impacts of global land cover change in the community climate system model," *International Journal of Climatology*, vol. 30, no. 13, pp. 2066–2087, 2010.
- [8] B. J. Strengers, C. Müller, M. Schaeffer et al., "Assessing 20th century climate-vegetation feedbacks of land-use change and natural vegetation dynamics in a fully coupled vegetation-climate model," *International Journal of Climatology*, vol. 30, no. 13, pp. 2055–2065, 2010.
- [9] K. P. Gallo, D. R. Easterling, and T. C. Peterson, "The influence of land use/land cover on climatological values of the diurnal temperature range," *Journal of Climate*, vol. 9, no. 11, pp. 2941–2944, 1996.
- [10] J. Hansen, R. Ruedy, M. Sato et al., "A closer look at United States and global surface temperature change," *Journal of Geophysical Research: Atmospheres*, vol. 106, no. 20, pp. 23947–23963, 2001.
- [11] L. Zhao, X. Lee, R. B. Smith, and K. Oleson, "Strong contributions of local background climate to urban heat islands," *Nature*, vol. 511, no. 7508, pp. 216–219, 2014.
- [12] Y. Sun, X. Zhang, G. Ren, F. W. Zwiers, and T. Hu, "Contribution of urbanization to warming in China," *Nature Climate Change*, vol. 6, no. 7, pp. 706–709, 2016.

- [13] N. B. Grimm, S. H. Faeth, N. E. Golubiewski et al., "Global change and the ecology of cities," *Science*, vol. 319, no. 5864, pp. 756–760, 2008.
- [14] Q. Li, H. Zhang, X. Liu, and J. Huang, "Urban heat island effect on annual mean temperature during the last 50 years in China," *Theoretical and Applied Climatology*, vol. 79, no. 3-4, pp. 165–174, 2004.
- [15] G. Y. Ren, Z.-Y. Chu, Z.-H. Chen et al., "Implications of temporal change in urban heat island intensity observed at Beijing and Wuhan stations," *Geophysical Research Letters*, vol. 34, no. 5, pp. 89–103, 2007.
- [16] Z. Yan, Z. Li, Q. Li, and P. Jones, "Effects of site change and urbanization in the Beijing temperature series 1977-2006," *International Journal of Climatology*, vol. 30, no. 8, pp. 1226–1234, 2010.
- [17] X. Yang, Y. Hou, and B. Chen, "Observed surface warming induced by urbanization in east China," *Journal of Geophysical Research*, vol. 116, no. 14, p. D14, 2011.
- [18] J. Wang, J. Feng, Z. Yan, Y. Hu, and G. Jia, "Nested high-resolution modeling of the impact of urbanization on regional climate in three vast urban agglomerations in China," *Journal of Geophysical Research: Atmospheres*, vol. 117, no. 21, 2012.
- [19] P. Yang, G. Ren, and W. Liu, "Spatial and temporal characteristics of Beijing urban heat island intensity," *Journal of applied meteorology and climatology*, vol. 52, no. 8, pp. 1803–1816, 2013.
- [20] J. Wang and Z.-W. Yan, "Urbanization-related warming in local temperature records: a review," *Atmospheric and Oceanic Science Letters*, vol. 9, no. 2, pp. 129–138, 2016.
- [21] S. Lin, J. Feng, J. Wang, and Y. Hu, "Modeling the contribution of long-term urbanization to temperature increase in three extensive urban agglomerations in China," *Journal of Geophysical Research: Atmospheres*, vol. 121, no. 4, pp. 1683–1697, 2016.
- [22] A. J. Arnfield, "Two decades of urban climate research: a review of turbulence, exchanges of energy and water, and the urban heat island," *International Journal of Climatology*, vol. 23, no. 1, pp. 1–26, 2003.
- [23] I. D. Stewart, "A systematic review and scientific critique of methodology in modern urban heat island literature," *International Journal of Climatology*, vol. 31, no. 2, pp. 200–217, 2011.
- [24] E. Kalnay and M. Cai, "Impact of urbanization and land-use change on climate," *Nature*, vol. 423, no. 6939, pp. 528–531, 2003.
- [25] L. Bounoua, P. Zhang, G. Mostovoy et al., "Impact of urbanization on US surface climate," *Environmental Research Letters*, vol. 10, no. 8, article 084010, 2015.
- [26] J.-M. Feng, Y.-L. Wang, and Z.-G. Ma, "Long-term simulation of large-scale urbanization effect on the east Asian monsoon," *Climatic Change*, vol. 129, no. 3-4, pp. 511–523, 2013.
- [27] E. Kalnay, M. Cai, H. Li, and J. Tobin, "Estimation of the impact of land-surface forcings on temperature trends in eastern United States," *Journal of Geophysical Research*, vol. 111, no. 6, article D06106, 2006.
- [28] M. N. Nuñez, H. H. Ciapessoni, A. Rolla, E. Kalnay, and M. Cai, "Impact of land use and precipitation changes on surface temperature trends in Argentina," *Journal of Geophysical Research*, vol. 113, no. 6, article D06111, 2008.
- [29] S. Nayak and M. Mandal, "Impact of land-use and land-cover changes on temperature trends over Western India," *Current Science*, vol. 102, no. 8, pp. 1166–1173, 2012.
- [30] Y. K. Lim, M. Cai, E. Kalnay, and L. Zhou, "Observational evidence of sensitivity of surface climate changes to land types and urbanization," *Geophysical Research Letters*, vol. 32, no. 22, pp. 117–137, 2005.
- [31] L. Zhou, R. E. Dickinson, Y. Tian et al., "Evidence for a significant urbanization effect on climate in China," *Proceedings of the National Academy of Sciences*, vol. 101, no. 26, pp. 9540–9544, 2004.
- [32] Y. Li, L. Zhu, X. Zhao, S. Li, and Y. Yan, "Urbanization impact on temperature change in China with emphasis on land cover change and human activity," *Journal of Climate*, vol. 26, no. 22, pp. 8765–8780, 2013.
- [33] Q. Wang, D. Riemann, S. Vogt, and R. Glaser, "Impacts of land cover changes on climate trends in Jiangxi province China," *International Journal of Biometeorology*, vol. 58, no. 5, pp. 645–660, 2013.
- [34] D. Zhou, S. Zhao, L. Zhang, and S. Liu, "Remotely sensed assessment of urbanization effects on vegetation phenology in China's 32 major cities," *Remote Sensing of Environment*, vol. 176, pp. 272–281, 2016.
- [35] M. Kanamitsu, W. Ebisuzaki, J. Woollen et al., "NCEP-DOE AMIP-II reanalysis (R-2)," *Bulletin of the American Meteorological Society*, vol. 83, no. 11, pp. 1631–1644, 2002.
- [36] E. Kalnay, M. Kanamitsu, R. Kistler et al., "The NCEP/NCAR 40-year reanalysis project," *Bulletin of the American Meteorological Society*, vol. 77, no. 3, pp. 437–471, 1996.
- [37] J. Y. Liu, M. L. Liu, D. F. Zhuang et al., "Study on spatial pattern of land-use change in China during 1995-2000," *Science China Earth Sciences*, vol. 46, no. 4, pp. 373–384, 2003.
- [38] J. Liu, Z. Zhang, X. Xu et al., "Spatial patterns and driving forces of land use change in China during the early 21st century," *Journal of Geographical Sciences*, vol. 20, no. 4, pp. 483–494, 2010.
- [39] J. Liu, W. Kuang, Z. Zhang et al., "Spatiotemporal characteristics, patterns, and causes of land-use changes in China since the late 1980s," *Journal of Geographical Sciences*, vol. 24, no. 2, pp. 195–210, 2014.
- [40] State Forestry Administration of the People's Republic of China, *China Forestry Statistical Yearbook*, China Forestry Publishing House, Beijing, China, 2001–2010.
- [41] G. B. Bonan, "Effects of land use on the climate of the United States," *Climatic Change*, vol. 37, no. 3, pp. 449–486, 1997.
- [42] D. Baldocchi, F. M. Kelliher, T. A. Black et al., "Climate and vegetation controls on boreal zone energy exchange," *Global Change Biology*, vol. 6, no. 1, pp. 69–83, 2010.
- [43] A. Buyantuyev and J. Wu, "Urban heat islands and landscape heterogeneity: linking spatiotemporal variations in surface temperatures to land-cover and socioeconomic patterns," *Landscape Ecology*, vol. 25, no. 1, pp. 17–33, 2009.
- [44] W. Kuang, W. Chi, D. Lu, and Y. Dou, "A comparative analysis of megacity expansions in China and the U.S.: patterns, rates and driving forces," *Landscape and Urban Planning*, vol. 132, pp. 121–135, 2014.
- [45] M. Wang, X. Zhang, and X. Yan, "Modeling the climatic effects of urbanization in the Beijing-Tianjin-Hebei metropolitan area," *Theoretical and Applied Climatology*, vol. 113, no. 3-4, pp. 377–385, 2012.
- [46] W. Kuang, Y. Liu, Y. Dou et al., "What are hot and what are not in an urban landscape: quantifying and explaining the land surface temperature pattern in Beijing, China," *Landscape Ecology*, vol. 30, no. 2, pp. 357–373, 2014.
- [47] C. Y. Sun, Q. Q. Shao, J. Y. Liu et al., "Characteristics of air temperature change affected by urban expansion in China,"

- Climatic and Environmental Research*, vol. 16, no. 3, pp. 337–346, 2011, in Chinese.
- [48] J. Wang, C. Xu, M. Hu et al., “A new estimate of the China temperature anomaly series and uncertainty assessment in 1900-2006,” *Journal of Geophysical Research: Atmospheres*, vol. 119, no. 1, pp. 1–9, 2014.
- [49] K. Jin, F. Wang, D. Chen et al., “Assessment of urban effect on observed warming trends during 1955-2012 over China: a case of 45 cities,” *Climatic Change*, vol. 132, no. 4, pp. 631–643, 2015.
- [50] C. Sun, Q. Shao, and J. Liu, “Application analysis of surface air temperature change estimation methods in Chinese mainland,” *Geo-information Science*, vol. 14, no. 1, pp. 14–21, 2012, in Chinese.
- [51] W. Liao, D. Wang, X. Liu, G. Wang, and J. Zhang, “Estimated influence of urbanization on surface warming in Eastern China using time-varying land use data,” *International Journal of Climatology*, vol. 37, pp. 3197–3208, 2016.



Hindawi

Submit your manuscripts at
www.hindawi.com

